

A Dynamic Macroscopic Framework for Pricing of Ride-hailing Services with an Optional Bus Lane Access for Pool Vehicles

Lynn Fayed¹ and Gustav Nilsson¹ and Nikolas Geroliminis¹

Abstract—On-demand trip sharing is an efficient solution to mitigate the negative impact e-hailing has on congestion. It motivates platform operators to reduce their fleet size, and serves the same demand level with a lower effective distance traveled. Users nevertheless prefer to travel solo and for shorter distances despite the fare discount they receive. By offering them the choice to pool and travel in high occupancy dedicated bus lanes, we provide them with a larger incentive to share their rides, yet this creates additional bus delays. In this work, we develop dynamic feedback-based control schemes that adjust the price gap between solo and pool trips to improve multi-modal delays. First, we develop a modal- and space-dependent aggregate model for private vehicles, ride-pooling, and buses, and we use this model to test different control strategies. To minimize the error between the target and actual speeds in the bus network, we design a PI controller and show that by adjusting pool trip fares, we can, with little input data, minimize this error. We also put forward a Model Predictive Control (MPC) framework to minimize the total Passenger Hours Traveled (PHT) and Waiting Times (WT) for the different travelers. Moreover, we show how the MPC framework can be utilized to impose a minimum speed in dedicated bus lanes to ensure that the buses operate on schedule. The results mark the possibility of improving the overall network conditions by incentivizing or discouraging pooling in the vehicle or bus network.

Index Terms—Macroscopic fundamental diagrams, Model predictive control, Multi-modal networks, Ride-hailing, Space allocation, Pricing

I. INTRODUCTION

The surge of on-demand mobility offers network commuters innovative transport alternatives for their trips. Characterized by their flexibility, convenience, and accessibility, on-demand modes have soon become widely popular, rooting their success in the fast-growing wireless communication technologies and the increasing interest in a more personalized mobility service. Ride-hailing, among many other similar modes, is nowadays a well-established transport alternative where a unique platform connects riders and drivers. Users request a ride, the request being most of the time instantaneous with no in-advance booking, and they are assigned to a nearby driver shortly after. The latter decides whether to carry users from their

origins to their destinations based on their relative evaluation of the trip attractiveness. While being as convenient as private vehicles due to their door-to-door services, these services usually prevail over public transportation because of their shorter waiting times before pick-up [2].

The burgeoning number of ride-hailing services and their wide success required authorities to impose incentive- or enforcement-based regulation strategies. These strategies are introduced to contain the negative impact that ride-hailing has on multi-modal urban traffic and user mode choice distribution. A closer look at the operation of ride-hailing services holds drivers accountable for the increase in traffic congestion [3]. More specifically, a high number of idling ride-hailing drivers not only causes an increase in congestion but also has a counterproductive effect by extending the waiting for users due to longer dispatching time despite the high availability of empty vehicles [4]. Moreover, the vast majority of current ride-hailing users reported that they would use public transportation if such services were not available, hence creating a direct competition with buses [5]. Clearly, the decline in the use of mass transit due to the shift in users' choice towards ride-hailing services raises multiple concerns about the undesired competition between these two modes.

To design well-informed and well-targeted policies, it is crucial to provide regulators with quantification studies that concretize the different impacts that ride-hailing has on the traffic externalities, the welfare of the drivers and riders, and the modal split between the different modes in a network [6]. This approach guides authorities to enforce appropriate actions to prevent further propagation of these services without proper regulations. A high fleet size, for instance, shortens the waiting time of users yet increases traffic congestion in urban spaces. One way to mitigate this is through sending empty vehicles with no assigned trip to available off-street parking locations [4], [7], [8] or to enforce a cap on the fleet size or the maximum allowable VKT carried out by the ride-hailing fleet [9]. Moreover, particularly when operating in a monopoly setting, ride-hailing platforms set a profit-maximizing fare without consideration of the rider's or driver's welfare. Many studies additionally investigated what the driver's wage and the rider's fare should be under a social welfare maximization framework. They argue that despite them not being sustainable from a revenue-maximization point of view, these pricing schemes are socially optimum when assessed in an equilibrium setting [10], [11].

Promoting trip sharing is another strategy to reduce the

¹The authors are with the Urban Transport Systems Laboratory (LUTS), École Polytechnique Fédérale de Lausanne (EPFL), Switzerland. {lynn.fayed,gustav.nilsson,nikolas.geroliminis}@epfl.ch

This work was supported by the Swiss National Science Foundation under NCCR Automation, grant agreement 51NF40_180545.

A preliminary version of some of the work in this paper was presented in [1].

total Vehicle Kilometers Travelled (VKT) by drivers to serve the same demand level [12]. It also allows the shrinking of the fleet size required to provide the same service level [13]. Generally referred to as ride-splitting or ride-pooling, this service prompts users to share their rides with other travelers in exchange for a fare discount to compensate for the extra detour incurred. Whether the passenger-to-passenger pool matching is successful depends on a myriad of factors, including the engagement levels in pooling, i.e., the willingness of users to share their rides with other users in the system, but also on their subsequent pick-up and drop-off locations [14]. In the scope of this work, however, we ignore the possibility of a failed passenger-to-passenger pool matching, and we assume that all requests opting for pooling will eventually be pooled. We also limit the trip sharing to two passengers, even if high-capacity on-demand micro-transit services are gaining fast momentum [14].

Having highlighted the importance of trip-sharing as a way to alleviate the negative externalities of ride-hailing services [15], these services are still attracting low to moderate demand levels. Therefore, we advance in this work an occupancy and space-dependent allocation strategy where pooling is motivated by allowing shared trips to use dedicated bus lanes. Although the majority of impact assessment and policy evaluation studies were formulated in a static equilibrium setting, we adopt in our framework a macroscopic dynamic approach with time-varying demand to capture the non-equilibrium and transient states of the network dynamics, and how the system evolves under different demand profiles during the day. More specifically, we tackle in this work the effect on multi-modal delays of incentivizing trip-sharing by entitling pool users to a spatial privilege or a higher fare discount. In the remaining part of the introduction, we provide a detailed overview of the relevant research tackling different aspects of our work, including i) the static and dynamic modeling of ride-hailing/ride-splitting and their service optimization, and ii) the status of ride-hailing with respect to the other more traditional operating modes in the network.

The common ground in any study tackling ride-hailing is to have a representative model capable of capturing the main features and characteristics of these services and the different stakeholders involved. The first insight into drawing the distinction between traditional taxi services and on-demand ride-hailing is to underline the appearance of a dispatching vehicle category that is non-existent in traditional taxi markets. It is the result of an online vehicle-passenger matching where the drivers' locations and the requests' origins are known to the platform [16]. Nevertheless, many studies have pointed out that, despite it sometimes being useful, online location access is a source of market inefficiency in the event of a demand surge where available vehicles are quickly depleted [17], [18]. A solution to this inefficiency is setting a surge pricing scheme that guarantees that the occurrence of these scenarios is avoided [19], even if this solution raises concerns about passengers' welfare. Service pricing is therefore an important element in ride-hailing modeling, thus justifying the large body of research investigating optimal full rider fare for ride-hailing [10] and optimal discounted fare for ride-splitting [11],

[20]. Similarly, [21] assessed service pricing but in a dynamic non-equilibrium setting with consideration of background traffic. Due to the spatial heterogeneity of demand and supply, it was also necessary to extend this framework to include a space-dependent pricing scheme balancing demand and supply in multi-regions, therefore guaranteeing a more efficient service level [22], [23]. Dynamic idle vehicle rebalancing strategies are also able to achieve the same outcomes but require having an accurate prediction of the demand in every region [24], [25].

The research line we describe particularly focused on modeling ride-hailing services, and very few accounted for on-demand trip-sharing in their framework. This is mainly because microscopically modelling trip-sharing, which is one of the main contributions of this work, is complex to conduct, especially when the number of passengers participating in a trip exceeds two. The focus hence deviated towards finding some empirical and universal laws for driver and passenger detours [26] or to assessing the different factors influencing the quality of a pooled trip [27]. Moreover, the passenger-to-passenger matching and the vehicle dispatching require advanced exact algorithms or heuristics to solve them in real-time settings [28], [13], [29], [30], even if in some work on two passenger-pooling, passenger-to-passenger matching probability prediction returned similar results to simulation settings [31]. Consequently, this computational effort makes it complex to integrate the matching with upper-level optimization problems like vehicle rebalancing or dynamic lane usage as in our case.

Positioning ride-hailing attractiveness relative to public transportation leads to questioning whether these two services are complementary or substitutionary. In areas where public transit is well-developed, ride-hailing is rather viewed as a first/last-mile solution complementing bus or metro services [32]. However, this does not eliminate the potential competition between the two modes where, in many cases, ride-hailing substitutes transit, hence causing an inevitable increase in the total VKT [6]. This observation led many researchers to formulate user equilibrium under different available alternatives where users have the choice to use ride-hailing either for their full trips or for a subpart of their trips [33], [34], [35]. They showed that subsidizing ride-hailing as a first/last-mile solution can indeed reinforce modal complementarity, despite reducing ride-hailing profit.

The purpose of this work is to assess the importance of ride-hailing in a multi-modal context and to advance an adaptive pricing strategy which, combined with an adequate spatial allocation scheme, allows us to minimize total delays in the network. This occupancy- or modal-dependent space allocation framework has been previously studied in the context of High-Occupancy Toll (HOT) lanes [36], [37] or dedicated lanes for Autonomous Vehicles (AV) on the link level [38], or for buses on the network level [39]. To the best of our knowledge, however, no work on modal- and occupancy-dependent allocation strategy to minimize overall network delays has considered ride-hailing services in its framework. The strategy we propose in this work was previously evaluated in a static setting, and network equilibrium solutions were

computed. The foremost result in this direction pointed out the need for a dynamic control framework to regulate priority lane usage for varying demand [40].

The contribution of this work is twofold. First, we build a dynamic macroscopic multi-modal dynamic model that utilizes Macroscopic Fundamental Diagrams (MFD) [41] to determine the dynamics of private vehicles, bus users, and ride-hailing services. We assume that ride-hailing users can choose to travel solo in the vehicle network or to pool in the bus network. In contrast to [1], we additionally consider the option of pooling in the vehicle network. Second, we introduce a regulatory pricing scheme for the pooling options and use the dynamic model developed within a control framework to determine what should the additional discount/fare that must be given/taken from pooling users be to steer the system toward its optimum. In other words, we propose a solution that minimizes the total delays and waiting times for all mode users in the network by adjusting the fares for pooled trips. Moreover, to guarantee minimal disturbances to buses, we impose a minimum speed in the bus network. This step ensures that buses continue to operate on schedule such that the utilization of their network by pool ride-hailing vehicles does not cause them significant delays.

The remainder of the paper is organized as follows. In the following section, Section II, we describe the modal- and occupancy-dependent space allocation strategy we present in this work, and elaborate on the macroscopic state dynamics for the different transportation modes using the network under assessment. Next, in Section III, we lay out the different control frameworks used for the purpose of improving network delays. To demonstrate the performance of the different controllers, we display the results of the simulations we run in Section IV. The paper finally concludes with the main findings and future directions in Section V.

II. MACROSCOPIC MULTI-MODAL FRAMEWORK

In the following section, we describe our macroscopic modelling framework by delineating the modal-dependent allocation strategy we propose. Next, we put forward the aggregate traffic model according to the spatial allocation policy advanced, and use it to define the traffic dynamics for the different transportation modes under consideration. The entire modeling framework is summarized in Figure 1.

A. Modal-dependent Space Allocation

In the network under consideration, travelers perform their trips using one of the available transportation alternatives in the set \mathcal{M} : private vehicles pv , buses b , and ride-hailing services rs such that $\mathcal{M} := \{pv, b, rs\}$. The dynamics for each alternative are modeled in discrete time with time step $k \in \mathcal{K} := \{0, \dots, k_{\max}\}$, and the duration of each time step is $\tau > 0$. Moreover, we let $\bar{\mathcal{K}} := \mathcal{K} \setminus \{k_{\max}\}$. Every transportation mode under consideration has an exogenous and time-dependent demand $Q_j(k)$ for $j \in \mathcal{M}$ expressed in passengers per hour. Commuters who opt for the ride-hailing alternative choose to either travel solo or to pool their trips with other users of the service. In terms of space utilization, private

vehicles perform their trips in the subspace of the network occupying a fixed fraction $\alpha \in [0, 1]$ of the total network space. Buses from their sides solely travel in dedicated bus lanes spanning over a fraction $1 - \alpha$ of the total space. We denote the vehicle and bus networks by \mathcal{V} and \mathcal{B} respectively, such that the set of available subnetworks is $\mathcal{N} := \{\mathcal{V}, \mathcal{B}\}$. Finally, if ride-hailing users opt for travelling solo, then the entirety of their trip is performed in the vehicle network \mathcal{V} . If however ride-hailing users choose to pool, they are granted the opportunity to either travel in the vehicle network \mathcal{V} or the bus network \mathcal{B} . This implies that the drivers of the ride-hailing fleet $N > 0$, assumed to be time-independent in our framework, can exclusively be in one of the following states:

- (i) driving an empty vehicle in the vehicle network \mathcal{V} , where the total number of drivers in this state is denoted by n_e ,
- (ii) delivering a solo trip in the vehicle network \mathcal{V} , where the total number of drivers in this state is denoted by n_s ,
- (iii) delivering a pool trip in the vehicle network \mathcal{V} , where the total number of drivers in this state is denoted by $n_p^{\mathcal{V}}$ and,
- (iv) delivering a pool trip in the bus network \mathcal{B} , where the total number of drivers in this state is denoted by $n_p^{\mathcal{B}}$.

It should be noted that we consider all of the aggregate states to be non-negative and continuous.

Moreover, let n_{pv} be the number of private vehicles in the vehicle network \mathcal{V} and n_b the number of buses in the bus network \mathcal{B} . Having defined the different vehicle categories, we know that the ride-hailing fleet at any time step $k \in \mathcal{K}$, under the assumption of a fixed fleet size, has to satisfy $N = n_e(k) + n_s(k) + n_p^{\mathcal{V}}(k) + n_p^{\mathcal{B}}(k)$. The accumulation in the vehicle network $n_{\mathcal{V}}$ at any time step $k \in \mathcal{K}$ is $n_{\mathcal{V}}(k) = n_{pv}(k) + n_e(k) + n_s(k) + n_p^{\mathcal{V}}(k)$, and the accumulation in the bus network $n_{\mathcal{B}}$ at any time step $k \in \mathcal{K}$ is $n_{\mathcal{B}}(k) = n_b + n_p^{\mathcal{B}}(k)$. Note that the number of operating buses in \mathcal{B} is assumed to be time-independent in our framework.

B. Aggregate traffic flow model

In the following part, we elaborate on the aggregate traffic model we use to estimate the speed in the vehicle and bus networks, i.e., \mathcal{V} and \mathcal{B} . Let $P : \mathbb{R}_{\geq 0} \rightarrow \mathbb{R}_{\geq 0}$ denote the full network production function without any dedicated bus lanes. The production P is dependent on the full network accumulation $n(k)$, for $k \in \mathcal{K}$, and can be calculated using the running network speed $v : \mathbb{R}_{\geq 0} \rightarrow \mathbb{R}_{\geq 0}$ such that $P(n(k)) = n(k)v(n(k))$. Following [42], [43], we can compute the define $P_{\mathcal{V}} : \mathbb{R}_{\geq 0} \rightarrow \mathbb{R}_{\geq 0}$ in the vehicle network and the production $P_{\mathcal{B}} : \mathbb{R}_{\geq 0} \rightarrow \mathbb{R}_{\geq 0}$ in the bus network using the space allocation factor α such that $P_{\mathcal{V}}(\alpha n(k)) = \alpha P(n(k))$ and $P_{\mathcal{B}}(\bar{\alpha} n(k)) = \bar{\alpha} P(n(k))$ where $\bar{\alpha} = 1 - \alpha$.

The relationship between production and accumulation is valid as long as the vehicles commuting in the bus network are standard vehicles. However, since buses perform frequent stops to board and alight passengers, they slow down the remaining vehicles utilizing the same space. To capture this interaction between buses and pooling vehicles utilizing the bus network, we partition the production in the bus network into pool vehicles production $P_p : \mathbb{R}_{\geq 0} \times \mathbb{R}_{\geq 0} \rightarrow \mathbb{R}_{\geq 0}$ and

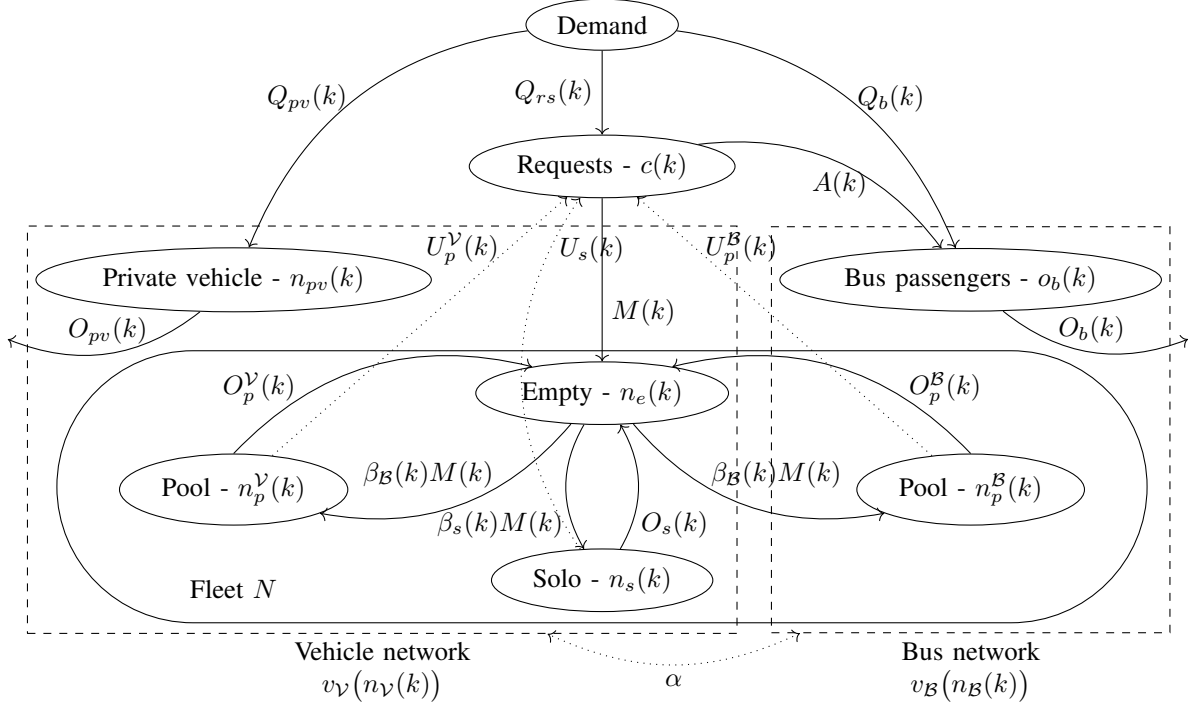


Fig. 1. A schematic sketch of the model under consideration. Private vehicles, empty ride-hailing vehicles, solo trips, and a portion of pool ride-hailing trips drive in the vehicle subnetwork \mathcal{V} , whereas buses and the remaining pool trip portion perform their trips in the bus subnetwork \mathcal{B} .

bus production $P_b : \mathbb{R}_{\geq 0} \times \mathbb{R}_{\geq 0} \rightarrow \mathbb{R}_{\geq 0}$, each dependent on both the number of pooling vehicles n_p^B and the number of buses n_b to obtain a 3D-MFD [44].

Analogous to the reasoning behind the split of the production function, the same applies here to the aggregate estimation of the speed in the vehicle network $v_{\mathcal{V}} : \mathbb{R}_{\geq 0} \rightarrow \mathbb{R}_{\geq 0}$ and bus network $v_{\mathcal{B}} : \mathbb{R}_{\geq 0} \rightarrow \mathbb{R}_{\geq 0}$ where $v_{\mathcal{V}}(\alpha n(k)) = v(n(k))$ and $v_{\mathcal{B}}(\bar{\alpha} n(k)) = v(n(k))$. Having estimated the individual speed function for every subnetwork, the production value in the vehicle network \mathcal{V} at time step $k \in \mathcal{K}$ is hence given by $P_{\mathcal{V}}(n_{\mathcal{V}}(k)) = n_{\mathcal{V}}(k)v_{\mathcal{V}}(n_{\mathcal{V}}(k))$ and that in the bus network \mathcal{B} is given by $P_{\mathcal{B}}(n_{\mathcal{B}}(k)) = n_{\mathcal{B}}(k)v_{\mathcal{B}}(n_{\mathcal{B}}(k))$. However, for the latter function, we account for the influence of buses on the vehicle speed by reducing $v_{\mathcal{B}}$ with a factor $r(n_b)$ dependent on the number of buses in the network where $r : \mathbb{R}_{\geq 0} \rightarrow (0, 1]$ and $\frac{dr}{dn_b} < 0$. Therefore, the actual speed of pool vehicles, that we denote by $v_p : \mathbb{R}_{\geq 0} \times \mathbb{R}_{\geq 0} \rightarrow \mathbb{R}_{\geq 0}$, is given by $v_p(n_p^B(k), n_b) = v_{\mathcal{B}}(n_{\mathcal{B}}(k))r(n_b)$. Regarding the bus operating speed that we denote $v_b : \mathbb{R}_{\geq 0} \times \mathbb{R}_{\geq 0} \rightarrow \mathbb{R}_{\geq 0}$, it must account for the repetitive stops that buses perform at stations such that

$$v_b(n_p^B(k), n_b) = \left(\frac{1}{1 + v_p(n_p^B(k), n_b) \frac{\bar{t}_d}{\bar{s}}} \right) v_p(n_p^B(k), n_b), \quad (1)$$

where \bar{t}_d and \bar{s} are the average bus dwell time and the spacing between bus stops respectively. It follows that the pool vehicle production in \mathcal{B} at time step $k \in \mathcal{K}$ is $P_p(n_p^B(k), n_b) = n_p^B(k)v_p(n_p^B(k), n_b)$ and the bus production is $P_b(n_p^B(k), n_b(k)) = n_b v_b(n_p^B(k), n_b)$.

The aggregate network-dependent production functions are used to estimate the trip completion rate –or outflow– for

every category of vehicles under consideration. While this approximation does not provide the same level of accuracy compared to trip-based models, it still allows a tractable analysis compared to the latter which is too complex for this sort of application [43]. As a result, in the following subsections, we utilize the production-based multi-modal macroscopic traffic model to estimate the changes as a function of time of the private vehicle accumulation, ride-hailing fleet assignment, and bus occupancy.

C. Network dynamics

Previously, we have defined the modal-dependent space allocation strategy and the subnetwork-dependent macroscopic traffic functions. In the following part, we elaborate on the aggregate dynamics of private vehicles, ride-hailing fleet, and bus average occupancies according to the proposed allocation strategy. Starting with the private vehicle category, the accumulation n_{pv} is computed using

$$n_{pv}(k+1) = n_{pv}(k) + \tau \left[\frac{Q_{pv}(k)}{\bar{o}_{pv}} - O_{pv}(k) \right], \quad \forall k \in \bar{\mathcal{K}}, \quad (2)$$

where $\bar{o}_{pv} > 0$ is the average occupancy of a private vehicle and $O_{pv}(k)$ is the trip completion rate computed using

$$O_{pv}(k) = \frac{n_{pv}(k) P_{\mathcal{V}}(n_{\mathcal{V}}(k))}{n_{\mathcal{V}}(k) \bar{l}_{pv}}, \quad (3)$$

where $\bar{l}_{pv} > 0$ is the constant average trip distance between the origin-destination pairs of private vehicle users. Note that we assume a homogeneous mixture of private and ride-hailing vehicles.

Moving to the ride-hailing mode, the various available options have different travel costs. Based on the relative cost of each option, the users choose to travel solo in \mathcal{V} , to pool in \mathcal{V} , or to pool in \mathcal{B} . Therefore, we let u_s denote the disutility for traveling solo, $u_p^\mathcal{V}$ the disutility for pooling in the vehicle network, and $u_p^\mathcal{B}$ the disutility for pooling in bus lanes. The expressions of the different utilities at time step $k \in \mathcal{K}$ are

$$U_s(k) = \tilde{F}_s(k) + \kappa \frac{\bar{l}_s}{v_\mathcal{V}(n_\mathcal{V}(k))}, \quad (4a)$$

$$U_p^\mathcal{V}(k) = \tilde{F}_p^\mathcal{V}(k) + \kappa \frac{\bar{l}_s + \Delta l_p}{v_\mathcal{V}(n_\mathcal{V}(k))}, \quad (4b)$$

$$U_p^\mathcal{B}(k) = \tilde{F}_p^\mathcal{B}(k) + \kappa \frac{\bar{l}_s + \Delta l_p}{v_p(n_p^\mathcal{B}(k), n_b)}, \quad (4c)$$

where $\kappa > 0$ is the value of time, $\bar{l}_s > 0$ is the average trip length for a solo trip, and $\Delta l_p \geq 0$ is the pool detour distance that passengers incur in case they opt for pooling. The variable \tilde{F}_s is the fare for travelling solo in \mathcal{V} , $\tilde{F}_p^\mathcal{V}$ is the fare for pooling in \mathcal{V} , and $\tilde{F}_p^\mathcal{B}$ is the fare for pooling in \mathcal{B} . In this work, we assume that $\tilde{F}_s(k)$ is constant such that $\tilde{F}_s(k) = F_s$ for all $k \in \mathcal{K}$ where $F_s > 0$ is the solo trip fare set by the platform operator. On the contrary, if $F_p > 0$ is the pool trip fare set by operator, then $\tilde{F}_p^\mathcal{V}(k) = F_p + \phi_\mathcal{V}(k)$ and $\tilde{F}_p^\mathcal{B}(k) = F_p + \phi_\mathcal{B}(k)$ where $\phi_\mathcal{V}(k) \in \mathbb{R}$ and $\phi_\mathcal{B}(k) \in \mathbb{R}$ are the control fares for pooling in the vehicle network \mathcal{V} and bus network \mathcal{B} respectively. The control fares are introduced to steer the total network towards different objectives that we expand on in Section III. The relative values of each of the disutility functions are used to compute the modal share for every available ride-hailing alternative. Therefore, let $\beta_\mathcal{V} \in [0, 1]$ and $\beta_\mathcal{B} \in [0, 1]$ be the fraction of the total ride-hailing demand that will choose to pool in \mathcal{V} and \mathcal{B} respectively at time step $k \in \mathcal{K}$, then using a multinomial logit model, we have that

$$\beta_\mathcal{V}(k) = \frac{e^{-\mu U_p^\mathcal{V}(k)}}{e^{-\mu U_s(k)} + e^{-\mu U_p^\mathcal{V}(k)} + e^{-\mu U_p^\mathcal{B}(k)}}, \quad (5a)$$

$$\beta_\mathcal{B}(k) = \frac{e^{-\mu U_p^\mathcal{B}(k)}}{e^{-\mu U_s(k)} + e^{-\mu U_p^\mathcal{V}(k)} + e^{-\mu U_p^\mathcal{B}(k)}}, \quad (5b)$$

where $\mu > 0$ is the scale parameter. The portion of users choosing to go solo at time step $k \in \mathcal{K}$ is $\beta_s(k)$ such that $\beta_s(k) = 1 - \beta_\mathcal{V}(k) - \beta_\mathcal{B}(k)$.

For ease of implementation purposes, we reformulate the utility and mode choice functions to set apart the control and state variables. Consequently, if we redefine the disutilities of the three available ride-hailing alternatives, excluding the controllable price changes, by u_s , $u_p^\mathcal{V}$, and $u_p^\mathcal{B}$, we get that

$$u_s(k) = F_s + \kappa \frac{\bar{l}_s}{v_\mathcal{V}(n_\mathcal{V}(k))}, \quad (6a)$$

$$u_p^\mathcal{V}(k) = F_p + \kappa \frac{\bar{l}_s + \Delta l_p}{v_\mathcal{V}(n_\mathcal{V}(k))}, \quad (6b)$$

$$u_p^\mathcal{B}(k) = F_p + \kappa \frac{\bar{l}_s + \Delta l_p}{v_p(n_p^\mathcal{B}(k), n_b)}, \quad (6c)$$

and if we set $\xi_\mathcal{V}(k)$ and $\xi_\mathcal{B}(k)$ as two variables that are function of $\phi_\mathcal{V}(k)$ and $\phi_\mathcal{B}(k)$ for all $k \in \mathcal{K}$, we get

$$\xi_\mathcal{V}(k) := e^{-\mu \phi_\mathcal{V}(k)}, \quad (7)$$

$$\xi_\mathcal{B}(k) := e^{-\mu \phi_\mathcal{B}(k)}. \quad (8)$$

Consequently, we can rewrite $\beta_\mathcal{V}(k)$ and $\beta_\mathcal{B}(k)$ as follows

$$\beta_\mathcal{V}(k) = \frac{\xi_\mathcal{V}(k) e^{-\mu u_p^\mathcal{V}(k)}}{e^{-\mu u_s(k)} + \xi_\mathcal{V}(k) e^{-\mu u_p^\mathcal{V}(k)} + \xi_\mathcal{B}(k) e^{-\mu u_p^\mathcal{B}(k)}}, \quad (9)$$

$$\beta_\mathcal{B}(k) = \frac{\xi_\mathcal{B}(k) e^{-\mu u_p^\mathcal{B}(k)}}{e^{-\mu u_s(k)} + \xi_\mathcal{V}(k) e^{-\mu u_p^\mathcal{V}(k)} + \xi_\mathcal{B}(k) e^{-\mu u_p^\mathcal{B}(k)}}. \quad (10)$$

We conclude that if $c(k)$ is the number of customers waiting to be matched at time k for all $k \in \mathcal{K}$, then we know that the number of passengers choosing to travel solo is $c_s(k) = (1 - \beta_\mathcal{V}(k) - \beta_\mathcal{B}(k))c(k)$ and the number of passengers choosing to pool is $(\beta_\mathcal{V}(k) + \beta_\mathcal{B}(k))c(k)$. By resorting to a Cobb-Douglas meeting function, we compute the matching rate $M(k)$ at time step $k \in \mathcal{K}$ using

$$M(k) = a_0 n_e(k)^{\alpha_e} \left(c_s(k) + \frac{1}{2} c_p(k) \right)^{\alpha_c}, \quad (11)$$

where $a_0 > 0$, $\alpha_e > 0$, and $\alpha_c > 0$ are the Cobb-Douglas meeting function parameters. Note that a factor $\frac{1}{2}$ is added to c_p to model that every single pool trip consists of two passengers. Subsequently, we can compute the dynamics of empty vehicles n_e at any time step using

$$n_e(k+1) = n_e(k) + \tau \left[\frac{n_s(k)}{n_\mathcal{V}(k)} \frac{P_\mathcal{V}(n_\mathcal{V}(k))}{\bar{l}_s} + \frac{n_p^\mathcal{V}(k)}{n_\mathcal{V}(k)} \frac{P_\mathcal{V}(n_\mathcal{V}(k))}{\bar{l}_s + \Delta l_d} + \frac{P_p(n_p^\mathcal{B}(k), n_b)}{\bar{l}_s + \Delta l_d} - M(k) \right], \quad \forall k \in \bar{\mathcal{K}}. \quad (12)$$

where the first three elements of (12) represent the completion rate of solo trips $O_s(k) = \frac{n_s(k)}{n_\mathcal{V}(k)} \frac{P_\mathcal{V}(n_\mathcal{V}(k))}{\bar{l}_s}$, the completion rate of pool trips in \mathcal{V} $O_p^\mathcal{V}(k) = \frac{n_p^\mathcal{V}(k)}{n_\mathcal{V}(k)} \frac{P_\mathcal{V}(n_\mathcal{V}(k))}{\bar{l}_s + \Delta l_d}$, and the completion rate of pool trips in \mathcal{B} $O_p^\mathcal{B}(k) = \frac{P_p(n_p^\mathcal{B}(k), n_b)}{\bar{l}_s + \Delta l_d}$. The last element of (12) denotes the number of empty vehicles that are matched and have therefore exited this category. The variable $\Delta l_d \geq 0$ represents the driver detour, which is the additional distance traveled by drivers to perform a pool trip relative to a solo one.

Moving to the discretized dynamics of the solo vehicle category n_s , we get that

$$n_s(k+1) = n_s(k) + \tau \left[\beta_s(k) M(k) - \frac{n_s(k)}{n_\mathcal{V}(k)} \frac{P_\mathcal{V}(n_\mathcal{V}(k))}{\bar{l}_s} \right], \quad \forall k \in \bar{\mathcal{K}}. \quad (13)$$

Similarly, the discretized dynamics for the pool vehicle in \mathcal{V} category, $n_p^{\mathcal{V}}$, are given by

$$n_p^{\mathcal{V}}(k+1) = n_p^{\mathcal{V}}(k) + \tau \left[\beta_{\mathcal{V}}(k)M(k) - \frac{n_p^{\mathcal{V}}(k) P_{\mathcal{V}}(n_{\mathcal{V}}(k))}{n_{\mathcal{V}}(k) \bar{l}_s + \Delta l_d} \right], \quad \forall k \in \bar{\mathcal{K}}. \quad (14)$$

Finally, the discretized dynamics for the pool vehicles in \mathcal{B} , category, $n_p^{\mathcal{B}}$, are given by

$$n_p^{\mathcal{B}}(k+1) = n_p^{\mathcal{B}}(k) + \tau \left[\beta_{\mathcal{B}}(k)M(k) - \frac{P_p(n_p^{\mathcal{B}}(k), n_b)}{\bar{l}_s + \Delta l_d} \right], \quad \forall k \in \bar{\mathcal{K}}. \quad (15)$$

So far, we have defined the changes in the ride-hailing vehicles category. In a similar manner, the changes in the number of passengers in the queue waiting to be assigned are

$$c(k+1) = c(k) + \tau \left[Q_{r.s}(k) - (1 + \beta_{\mathcal{V}}(k) + \beta_{\mathcal{B}}(k))M(k) \right] - A(k), \quad \forall k \in \bar{\mathcal{K}}. \quad (16)$$

Note here that the $(1 + \beta_{\mathcal{V}}(k) + \beta_{\mathcal{B}}(k))M(k)$ represents the outflow of the waiting requests category. It accounts for the fact that a pool trip match requires taking out two passengers of this category compared to a solo trip match. Finally, the variable $A(k) \geq 0$ represents the number of abandoning requests due to long waiting periods before pick-up. Therefore, if the waiting tolerance of ride-hailing customers is given by w_{\max} , then we can estimate the number of abandoning requests using

$$A(k) = \max \left(c(k) - \frac{1}{k} \sum_{\tilde{k}=1}^k M(\tilde{k})w_{\max}, 0 \right), \quad \forall k \in \mathcal{K}. \quad (17)$$

The abandonment approximation in (17) first computes the theoretical queue length if the ride-hailing request waiting time is w_{\max} and the matching rate is the average over the previous time steps, and then subtracts this quantity from the current queue length $c(k)$. If the resulting quantity is less than 0, this implies that the service level is rather satisfactory. The abandoning requests will not disappear from the system, but will rather perform their trips using buses.

The dynamics of the third transportation mode, buses, are formulated in terms of changes in occupancy rather than changes in the number of vehicles. This is because we assume that the number of buses n_b traveling in the bus network \mathcal{B} is constant and their occupancy is time-dependent. Assuming a uniform bus occupancy o_b over the available fleet of buses n_b , the discretized dynamics of o_b are given by

$$o_b(k+1) = o_b(k) + \frac{\tau}{n_b} \left[Q_b(k) + A(k) - \frac{P_b(n_p^{\mathcal{B}}(k), n_b)}{\bar{l}_b} o_b(k) \right], \quad \forall k \in \bar{\mathcal{K}}, \quad (18)$$

where \bar{l}_b is the average trip length by bus. Note here that the abandoning ride-hailing requests at time step $k \in \mathcal{K}$, $A(k)$, are considered here as an additional demand for the bus occupancy category. The last term of (18) represents the bus passenger trip completion rate $O_b(k) = \frac{P_b(n_p^{\mathcal{B}}(k), n_b)}{\bar{l}_b} o_b(k)$.

In the next section, Section III, we elaborate on the ride-hailing pricing scheme that we set forth to reduce the multi-modal user delays by utilizing the dynamic model we previously described.

III. CONTROL FRAMEWORK

The objective of the space allocation model we advance in this work is to redistribute the network space over the available transportation modes. However, the choice of ride-hailing users to travel solo or to pool is not always aligned with the objective of improving the total delays in the network. Therefore, in this section, we develop a regulatory pricing scheme to ensure that allowing a fraction of pool trips in bus lanes does not worsen multi-modal user delays. To do so, we evaluate two different control strategies. The first one is a Proportional-Integral (PI) controller with the objective of keeping the bus network at a certain speed. The PI controller is myopic and only requires information about the speed in the bus network to compute the control prices. The second control strategy we evaluate is the Model Predictive Control (MPC) with the objective of minimizing the total travel time.

A. PI control

Because our strategy moves pool vehicles to bus lanes, it is crucial to ensure that the disturbances to bus users are minimized, all while improving the travel time for the remaining travelers. We do so by changing the values of the pool trip control fares $\phi_{\mathcal{B}}$ according to the difference between the actual bus speed in network \mathcal{B} and the target bus speed, which we denote by $\bar{v}_b > 0$. This difference is also referred to as the bus speed error. The choice of $\phi_{\mathcal{B}}$ as our control variable in the PI framework is justified by the direct effect this quantity has on the amount of trip pooling in the bus network. In addition, we keep track of the previous errors for the last $N_e \in \mathbb{N}$ time steps. As a consequence, if $\epsilon(k) := (\bar{v}_b - v_b(n_p^{\mathcal{B}}(k), n_b))$ defines the error term at time step k , then the expression for $\phi_{\mathcal{B}}$ at time step $k \in \mathcal{K}$ is

$$\phi_{\mathcal{B}}(k) = K_p \epsilon(k) + \frac{K_i}{N_e} \sum_{\tilde{k}=\max(k-(N_e+1), 0)}^{k-1} \epsilon(\tilde{k}), \quad (19)$$

where $K_p > 0$ and $K_i \geq 0$ are the constant proportional gain and integral gain. In the result section, we show how the two different parameters, K_p and K_i , affect the performance of the PI controller by bridging the gap between the actual and target bus speed. The drawback of the PI controller, however, is that it only takes into account the speed of buses irrespective of the other mode users. Next, we show how the MPC implementation is capable of circumventing this matter.

B. Model predictive control

Unlike the PI controller, the aim of the MPC framework is to improve the total network delays using our proposed strategy. We quantify delays using the total Passenger Hours Travelled (PHT) of multi-modal users at any time step $k \in \mathcal{K}$, here equal to $\text{PHT}(k) = \tau [n_{pv}(k)\bar{o}_{pv} + n_b o_b(k) + n_s(k) + (n_p^{\mathcal{V}}(k) + n_p^{\mathcal{B}}(k))\bar{o}_p]$ and the total Waiting Time (WT) of ride-hailing requests at time step $k \in \mathcal{K}$, which is given by $\text{WT}(k) = \tau c(k)$. Therefore, the formulation of the MPC framework is given by

$$\begin{aligned} & \text{minimize} && \sum_{k \in \mathcal{K}} \text{PHT}(k) + \text{WT}(k) \\ & \text{subject to} && \xi_i(k) \in [\xi_{\min}, \xi_{\max}] \quad \forall k \in \mathcal{K}, \forall i \in \mathcal{N} \\ & && \xi_i(k) = \xi_i(k+1) \quad \forall k \in \bar{\mathcal{K}} \setminus \{n \cdot N_u \mid n \in \mathbb{N}\}, \\ & && \quad \quad \quad \forall i \in \mathcal{N} \end{aligned} \quad (20)$$

where ξ_{\min} and ξ_{\max} are the exogenous lower and upper bound of the control variable, \bar{o}_p is the average occupancy of a pool trip such that $\bar{o}_p \in (1, 2]$. The second constraint of (20) makes sure that the control actions are only updated every $N_u \in \mathbb{N}$ time steps. This avoids frequent fluctuations in the service pricing of ride-hailing, which is desirable from a user perspective.

IV. NUMERICAL STUDY

In the following section, we perform a numerical study to evaluate the impact of our proposed allocation scheme and we show the influence of different control strategies on the overall network performance. To do so, we describe in Subsection IV-A the simulation parameters that we utilize for illustration purposes. Next, in Subsections IV-B and IV-C, we assess network delays for scenarios with and without abandonment respectively. We do so to observe the impact of adding a ride-hailing user waiting tolerance on the objective function value defined as the sum of overall user delays and on-demand user waiting time.

A. Macro-simulation parameters

Next, we describe the simulation environment that we implement to test the potential benefits of our proposed strategy along with the different control schemes. For this purpose, we consider a network characterized by an MFD that aggregates the microscopic traffic dynamics. Its functional form is given by the production function $P(n) = A_0 n^3 + B_0 n^2 + C_0 n$, $A_0 = 5.74 \cdot 10^{-9}$, $B_0 = -1.02 \cdot 10^{-3}$, and $C_0 = 36$ for $n \in [0, 58536]$. The fractional split α partitioning the full network space into a vehicle network and a bus network has a value equal to 0.8, and is usually an unalterable property of the infrastructure. The value of α yields two production functions for every subnetwork according to the relationship described in Section II. Transforming the obtained vehicle MFD into a three-dimensional bus MFD requires the multiplication of the speed with a reduction factor $r(n_b)$ such that $r(n_b) = e^{-6.5 \cdot 10^{-4} n_b}$. The resulting function described in

Subsection II-B allows the computation of the pool vehicles running speed in the bus network v_p . Similarly, the bus operating speed is straightforwardly obtained by factoring in the spacing \bar{s} between bus stations and the dwell time \bar{t}_d at stops where $\bar{s} = 0.8$ km, and $\bar{t}_d = 30$ s as shown in (1). With respect to the Cobb-Douglas meeting function that we adopt in (11), its constant parameters are equal to 0.025, 0.93, and 0.98 for a_0 , α_e , and α_c respectively. To estimate the outflow for every category of vehicle, we assume that the average trip length for private vehicles is equal to that of solo trips such that $\bar{l}_{pv} = \bar{l}_s = 3.86$ km. Since bus trips are generally longer than direct origin-destination trips, we consider that the average bus trip distance is $\bar{l}_b = 1.4\bar{l}_{pv}$. Similarly, pool trips are also longer than \bar{l}_s due to the additional detour that passengers/drivers have to incur. The value of this detour is generally dependent on the number of passengers willing to engage in pooling. For the scope of this analysis, however, we will assume that the detour remains constant such that $\Delta l_d = 0.7\bar{l}_s$ and $\Delta l_p = 0.15\bar{l}_s$. The integration of a demand-dependent detour value will be examined in future works. The average occupancies of the different types of vehicles are 1 and 1.5 for \bar{o}_s and \bar{o}_p respectively, as the driver is excluded from the occupancy count. With respect to the private vehicles' occupancy o_{pv} , we use a value of 1.2.

Moving to the multinomial logit model dictating the choice between solo and pooled trip, we consider a mode choice scale parameter $\mu = 1$, and a value of time $\kappa = 30$ CHF/hr. The static trip fares for solo F_s and for pool F_p are 5 and 4 CHF, respectively. We note here that these values usually change with the total ride-hailing demand. Since the objective of this study is to determine the value of $\phi_{\mathcal{V}}$ and $\phi_{\mathcal{B}}$ irrespective of the values of F_s and F_p , we discard the demand-dependent basic fare variations. The fleet size N remains constant over the full simulation framework and is set to 3500 vehicles. The simulation runs over six hours and is discretized such that the duration of every time step τ is equal to 6 s. The demand profile for private vehicles and ride-hailing is displayed in Figure 2(a) where the increase in demand starts at around 16:00 before it goes back to its original value at around 18:00. The demand for buses varies in a similar manner as also shown in Figure 2(b).

B. Multi-modal network delays without abandonment

The changes of the state variables for the network under consideration without any regulatory interventions are shown in Figure 3. Under this scenario, which we refer to as the no control scenario, the choice of users is solely dictated by the platform-set fares and the subnetworks' travel time. Note that we display here the simulation results with no abandonment, i.e., when w_{\max} is infinitely large or equivalently $A(k) = 0$ for all $k \in \mathcal{K}$. During peak hours, the accumulation of private vehicles n_{pv} spiraled up in Figure 3(a). With respect to the different states of the ride-hailing fleet size, it can be observed from Figures 3(b)-3(d), that the number of solo trip vehicles n_s and pool trip in \mathcal{B} vehicles $n_p^{\mathcal{B}}$ increased during peak hours whereas the number of pool trip in \mathcal{V} vehicles $n_p^{\mathcal{V}}$ remains almost constant after some initial transient behavior. The

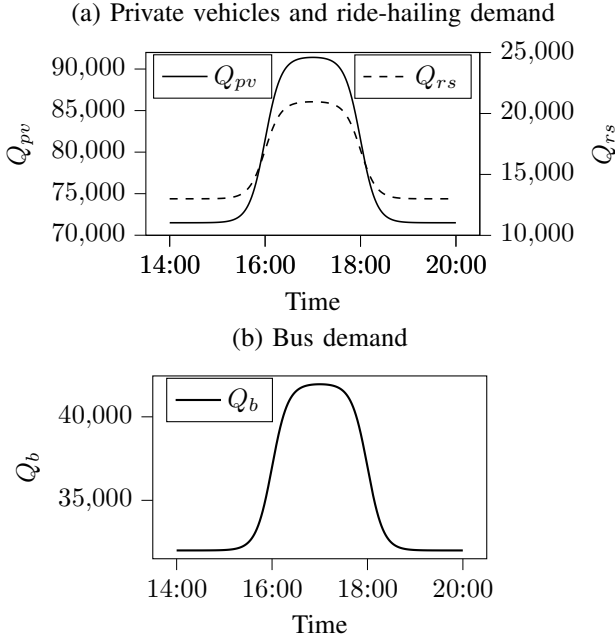


Fig. 2. Time-dependent multi-modal demand profile in pax/hr.

TABLE I
MACRO-SIMULATION RESULTS WITHOUT ABANDONMENT

Scenario	PHT+WT [pax.hr]	PHT [pax.hr]	WT [pax.hr]
$\beta_V = 0$ & $\beta_B = 0$	246980	193913	53067
$\beta_V \in [0, 1]$ & $\beta_B = 0$	239819	198116	41703
$\beta_V = 0$ & $\beta_B \in [0, 1]$	190872	176442	14430
$\beta_V = 0$ & $\beta_B = 1$	223210	188097	35113
$\beta_V \in [0, 1]$ & $\beta_B \in [0, 1]$	188954	177389	11565
PI control - ϕ_B	191383	178709	12674
MPC - ϕ_B	188316	176721	11595
MPC (\underline{v}_b) - ϕ_B	191464	178515	12949
MPC - ϕ_V and ϕ_B	187030	176348	10682
MPC (\underline{v}_b) - ϕ_V and ϕ_B	189725	178352	11373

deterioration of the condition in the vehicle network, reflected in the reduction in speed v_V in Figure 3(e), prompts the user to pool in the bus network. This is confirmed by looking at the increase in the share of pool users opting to travel in the bus network β_B and the decrease in the share of pool users opting to travel in the bus network β_V as seen in 3(h). The total delays for all users in the network for this specific scenario, i.e., when $\beta_V \in [0, 1]$ and $\beta_B \in [0, 1]$ are determined through (9) and (10) respectively, and are displayed in Table I, where, for $\beta_V \in [0, 1]$ and $\beta_B \in [0, 1]$, the sum of PHT and WT is equal to 188954 pax.hr.

To put the result above into context, we compare it with settings where the choices for the pooling users are limited. Table I shows the user delays for such scenarios. The worst performing scenario is when no pooling is involved, i.e., when both β_V and β_B are equal to zero. This is because for constant fleet sizes, solo travel results in longer queues and longer waiting times, especially when all ride-hailing vehicles are occupied and few vehicles are available for pick-up. When pooling is only allowed in the vehicle network, i.e., $\beta_B = 0$ and $\beta_V \in [0, 1]$, the total delays are much greater than the

TABLE II
MULTI-MODAL DELAYS WITHOUT ABANDONMENT

Scenario	PHT _{pv} [pax.hr]	PHT _{rs} [pax.hr]
$\beta_V = 0$ & $\beta_B = 0$	114856	18518
$\beta_V \in [0, 1]$ & $\beta_B = 0$	114856	22721
$\beta_V = 0$ & $\beta_B \in [0, 1]$	84623	20770
$\beta_V = 0$ & $\beta_B = 1$	75462	26713
$\beta_V \in [0, 1]$ & $\beta_B \in [0, 1]$	87991	21572
PI control - ϕ_B	89527	21798
MPC - ϕ_B	87355	21564
MPC (\underline{v}_b) - ϕ_B	91091	21631
MPC - ϕ_V and ϕ_B	87669	21186
MPC (\underline{v}_b) - ϕ_V and ϕ_B	91308	21459

TABLE III
BUS DELAYS

Scenario	PHT _b [pax.hr]	$n_b \int \max(\bar{v}_b - v_b, 0) dt$ [km]
$\beta_V = 0$ & $\beta_B = 0$	60539	0
$\beta_V \in [0, 1]$ & $\beta_B = 0$	60539	0
$\beta_V = 0$ & $\beta_B \in [0, 1]$	71049	2634
$\beta_V = 0$ & $\beta_B = 1$	85922	11869
$\beta_V \in [0, 1]$ & $\beta_B \in [0, 1]$	67825	958
PI control - ϕ_B	67384	90
MPC - ϕ_B	67802	1430
MPC (\underline{v}_b) - ϕ_B	65792	0
MPC - ϕ_V and ϕ_B	67493	1354
MPC (\underline{v}_b) - ϕ_V and ϕ_B	65584	0

scenario where pooling is only allowed in the bus network with $\beta_V = 0$. This is due to users opting for pooling in the bus network, causing ride-hailing vehicles to travel at a larger speed, and making them available soon after to perform a new trip. We note here that we also provide the simulation results for when $\beta_B = 1$ which implies $\beta_V = 0$, meaning that all ride-hailing users are pooling in the bus network. The reason for that is to show that this extreme solution causes significant delays for bus users and long waiting times, and is therefore not attractive at the system level. Motivated by these observations, the need to regulate the share of each ride-hailing alternative becomes more substantiated. For this reason, we resort to different controllers to find a proper pricing scheme that minimizes the observed delays.

1) *PI controller framework*: To guarantee that our allocation strategy does not worsen the situation for mainly bus users, we implement the PI control framework in our simulation and report the different state variables in Figure 8. The choice of the set point for the desired speed in the bus network, however, remains complex because bus users should ideally travel at the highest possible speed, and this speed is defined by the bus operator or the traffic regulators. In the results provided, we set \bar{v}_b to 17 km/hr while the default bus speed in the absence of cars is $v_b(0, n_b) = 19$ km/hr. This choice of set point ensures that the permissible decrease in bus speeds due to the bus lane usage remains within acceptable ranges.

The plots in Figure 8 show the system dynamics for different proportional and integral gain values K_p and K_i respectively, all with $N_e = 100$ time steps. The variations of n_{pv} , n_s , n_p^B , and n_p^V in Figures 8(a)-8(d) are almost similar to what is observed in Figures 3(a)-3(d), except for the lower number of

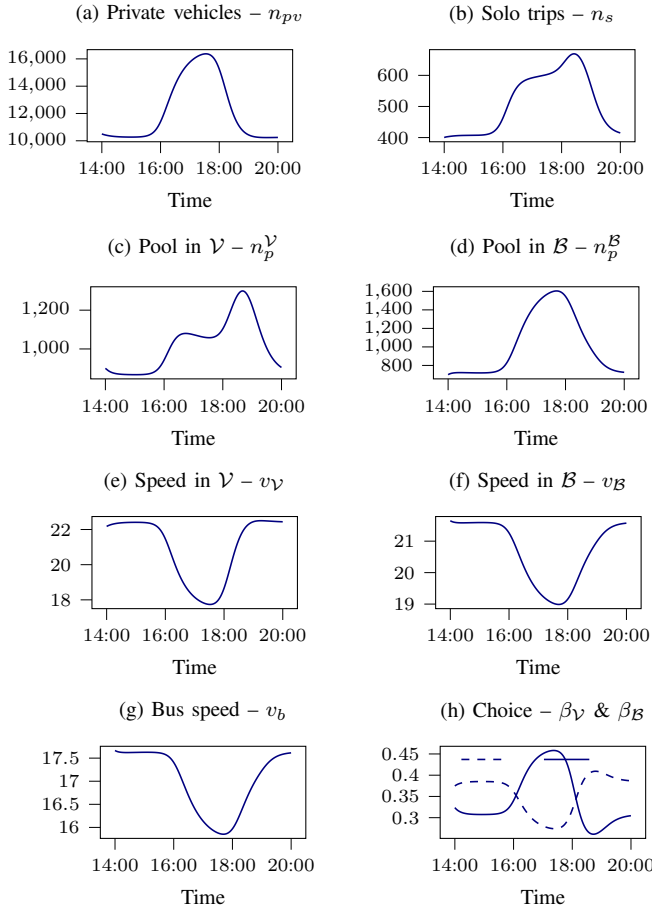


Fig. 3. Time-dependent model variables for the no control scenario without abandonment for (a) private vehicle accumulation, (b) solo trip ride-hailing vehicles, (c) pool trip ride-hailing accumulation in \mathcal{V} , (d) pool trip ride-hailing accumulation in \mathcal{B} , (e) speed in the vehicle network \mathcal{V} , (f) vehicle speed in the bus network \mathcal{B} , (g) bus speed in the bus network \mathcal{B} , and (h) fraction of pool trip in \mathcal{V} and \mathcal{B} respectively.

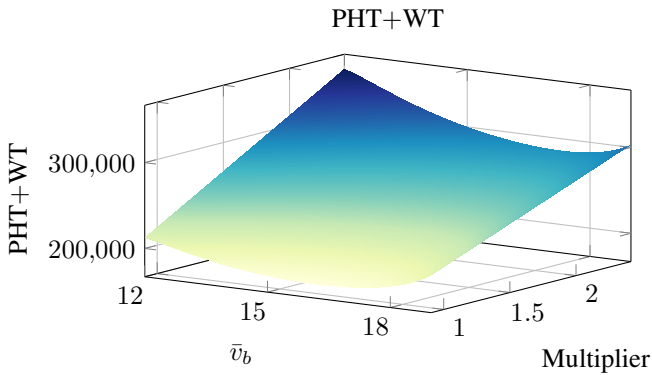


Fig. 4. Objective function values for different set points and different bus demand profiles under the PI control framework.

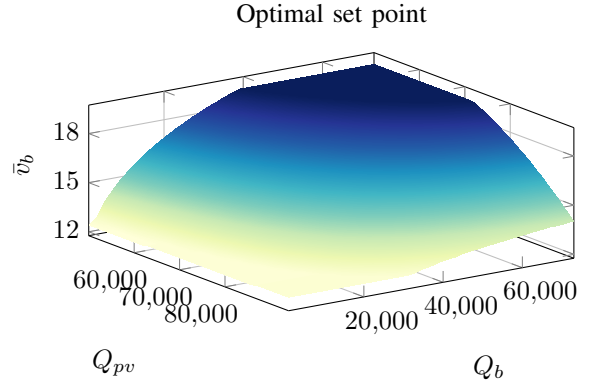


Fig. 5. Optimal PI bus speed set points for different private vehicles and bus demands.

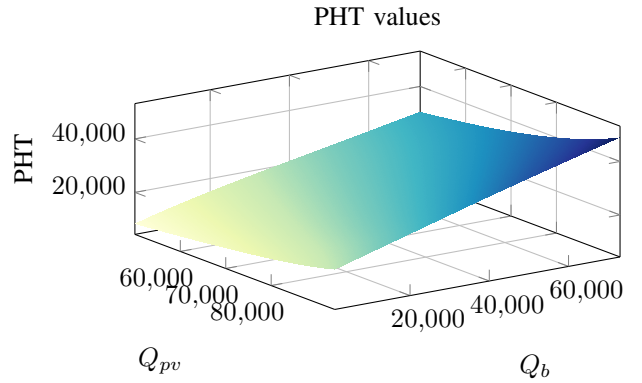


Fig. 6. PHT values for optimal set points.

solo trips and higher number of pool trips in \mathcal{B} , especially during off-peak period. This is because the bus network is significantly underutilized during off-peak hours, and its capacity allows for some ride-hailing users to pool their trips in \mathcal{B} . This justifies the exorbitantly high discount ϕ_B granted to users at the beginning of the simulation in Figure 8(i) to encourage them to pool their trips in \mathcal{B} . Note here that in the PI framework, we focus on controlling ϕ_B because it has a direct influence on the bus speed v_b . In other words, we set ϕ_V to 0 in our numerical experiment.

Moreover, we observe that picking reasonable values for K_p and K_i yields realistic pricing scenarios, all while achieving the desired objective of bridging the gap between the actual and target bus speeds as can be seen in Figure 8(i) compared to scenarios with no integral term. Due to the time-dependent nature of the demand in our simulations, the PI controller fails to achieve lower objective function values compared to the scenario with no control where the total delays are equal to 191383 and 188954 pax.hr, respectively. First, the dynamic nature of the problem implies that the choice of set points is not straightforward.

The approach we have adopted so far accounts for bus user delays without consideration of the overall network performance. Therefore, the previous choice of set point does not guarantee a convenient solution for all network users. In Figure 4, we display the value of PHT and WT for various PI

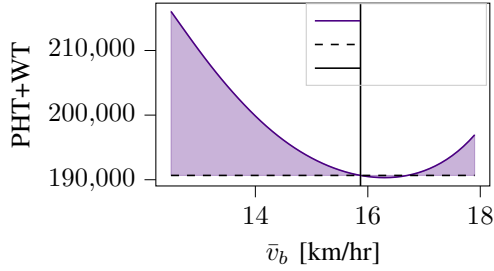


Fig. 7. Difference between the optimal static and dynamic bus speed set points for the PI controller.

set points and different on-peak period bus demand multipliers. The displayed results reflect that a lower \bar{v}_b is acceptable if the objective is to minimize multi-modal delays. A more practical way to determine this network operational point is to extend the static model developed in [40], and compute the value of bus speed at optimality for the pair of time-invariant private vehicles and bus demands. The results of this approach are shown in Figure 5. From the figure, we can see that for the current setting, the set-point is demand-dependent. The corresponding minimum PHT for the different demand combinations are shown in Figure 6. Since bus lanes usually occupy a small fraction of the network infrastructure, increasing bus demand has the most significant impact on the PHT values.

Figure 7 shows the variation of the PHT results for different choices of the PI controller set points for the bus demand profile in Figure 2(b), and compare them with the optimal set point found by solving the static formulation. Clearly, the value of \bar{v}_b minimizing delays does not fully coincide. Nevertheless, the static choice of \bar{v}_b gives some insights into what value is potentially able to minimize delays.

However, despite it being convenient from an implementation point of view, the formulation of the PI framework does not allow to explicitly achieve a multi-modal system optimum. Therefore, we broaden our formulation to include all network users by resorting to an MPC framework, and report the results for when the optimization framework runs with one control variable ϕ_B , and two control variables ϕ_V and ϕ_B .

2) *MPC framework*: The results of the different MPC implementations in Table I show that when our regulatory prices dictate the amount of pooling in both the vehicle and the bus network, we get the lowest objective function value. This is because trip pooling, even if performed in network \mathcal{V} , makes the ride-hailing vehicles available soon after for a new trip, hence reducing the waiting times of ride-hailing users. Note that even if we only consider one control variable ϕ_B , we already observe some improvements compared to the no control scenario. In fact, the results in Table I reveal that, in reference to the scenario with no control and no pooling in bus lanes, the MPC framework allows for 8% improvement compared to the PI implementation. In addition to the previous results, we also report the outcomes of the MPC with a lower bound \underline{v}_b on the minimum bus speed allowed in the bus network \mathcal{B} . We do so to guarantee that the bus services do not significantly lose performance, even if this implies

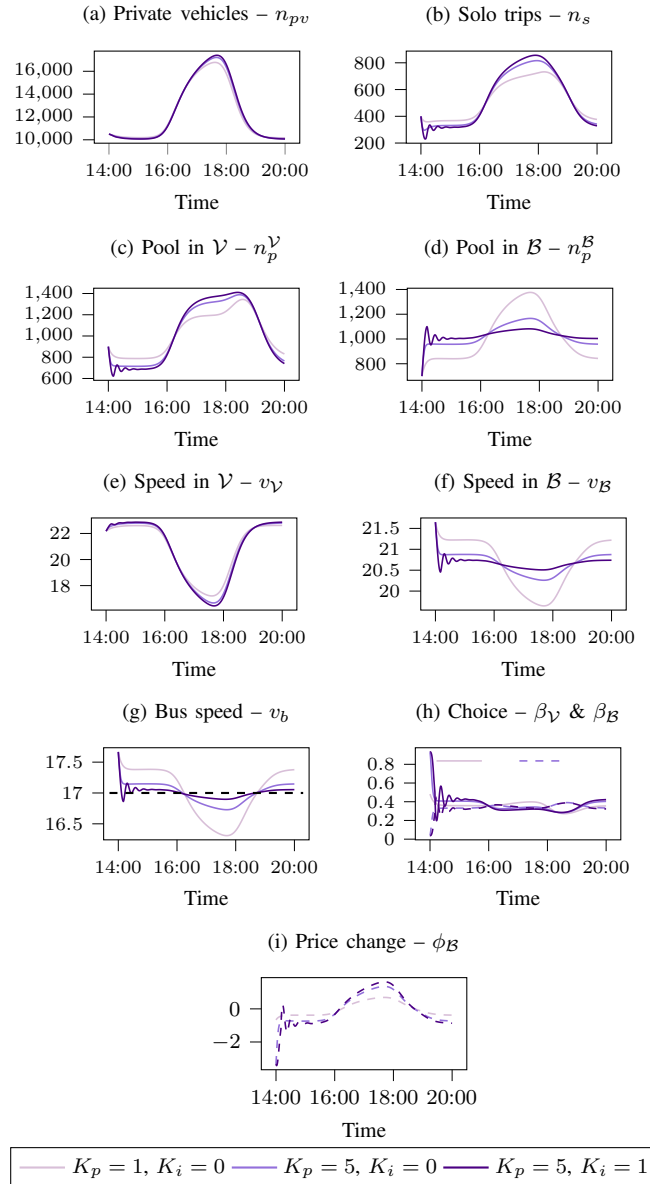


Fig. 8. Time-dependent model variables for the PI framework without abandonment for (a) private vehicle accumulation, (b) solo trip ride-hailing vehicles, (c) pool trip ride-hailing accumulation in \mathcal{V} , (d) pool trip ride-hailing accumulation in \mathcal{B} , (e) speed in the vehicle network \mathcal{V} , (f) vehicle speed in the bus network \mathcal{B} , (g) bus speed in the bus network \mathcal{B} , (h) fraction of pool trip in \mathcal{V} and \mathcal{B} respectively, and (i) regulatory control fare for pooling in \mathcal{B} .

a better total PHT for the overall network. Clearly, when the value of \underline{v}_b is set to 17 km/hr, the objective function value increases because the private vehicle and ride-hailing delays, that we denote by PHT_{pv} and PHT_{rs} , also increase as reported in Table II. However, when we numerically compute in Table III the bus delays PHT_b and the constraint violations of the minimum bus speed, we guarantee the public transit performance is minimally impacted.

To understand how the MPC framework influences the results, we display the variations of the main simulation variables in Figure 9. Note that for this simulation, we set ξ_{\min} and ξ_{\max} to be equal to e^{-3} and e^3 respectively. Moreover, for practicality reasons, we only allow the control variable to

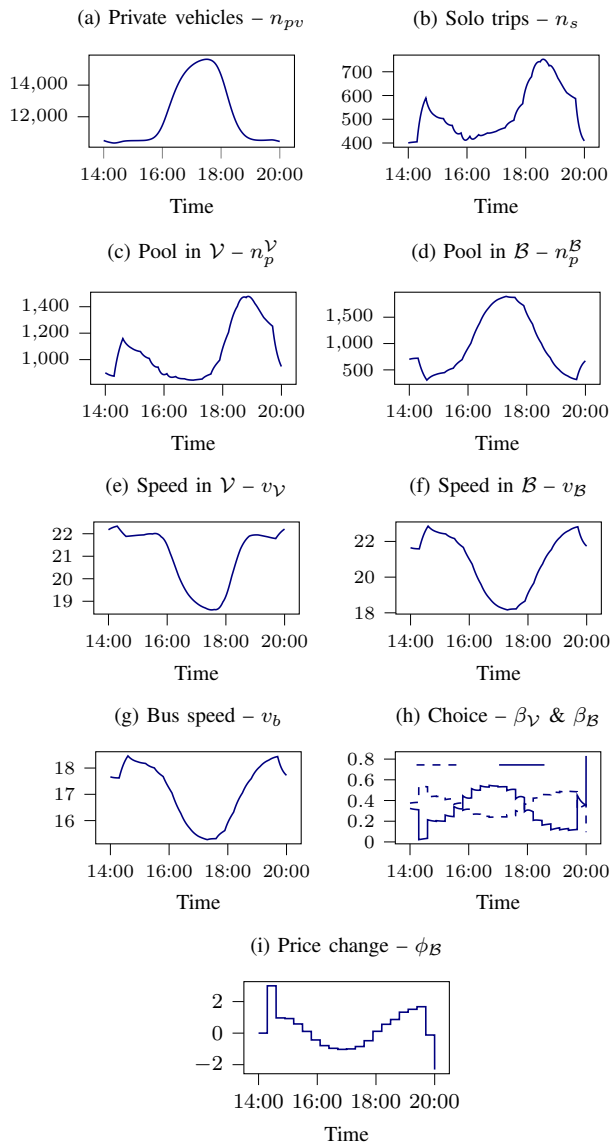


Fig. 9. Time-dependent model variables for the MPC framework without abandonment for (a) private vehicle accumulation, (b) solo trip ride-hailing vehicles, (c) pool trip ride-hailing accumulation in \mathcal{V} , (d) pool trip ride-hailing accumulation in \mathcal{B} , (e) speed in the vehicle network \mathcal{V} , (f) vehicle speed in the bus network \mathcal{B} , (g) bus speed in the bus network \mathcal{B} , (h) fraction of pool trip in \mathcal{V} and \mathcal{B} respectively, and (i) regulatory control fare for pooling in \mathcal{B} .

be updated every 180 time steps such that $N_u = 180$. As opposed to the PI controller, the MPC shows a more demand-responsive behavior where, during off-peak periods, the speed in the vehicle network in Figure 9(e) is lower than that in the bus network observed in Figure 9(f). This substantiates the relatively high values of ϕ_B as the use of the bus network is privileged in this case. During the on-peak period, however, ϕ_B becomes negative, implying that ride-hailing users in the vehicle networks are causing significant delays compared to bus users, and therefore encouraging people to pool their rides in bus lanes is necessary to reduce the total delays for multi-modal users.

C. Multi-modal network delays with abandonment

The results we reported so far display scenarios where the ride-hailing users never abandon their requested trip, regardless of the waiting time. Table IV shows the delays and abandonment values for when the ride-hailing users' waiting tolerance w_{\max} is set to 15 min. Irrespective of the scenario under consideration, the values of the objective function when abandonment is considered in the dynamic model are lower than the values with no abandonment in Table I. Again, for this case, the lowest objective function values are observed for the MPC implementation. In fact, when looking at the individual delays of multi-modal users in Table V, we notice that the MPC framework is capable of returning a solution that is convenient for all multi-modal users. We note here that due to the complexity of the abandonment function, the MPC dynamics are run without any abandoning requests, and the output control variables are then applied in the real settings dynamics with abandonment. Figure 10 describes the approach we follow when implementing the MPC. For each optimization run, we consider a prediction horizon of $\tilde{N} = 650$ time steps, i.e., we assume that the optimizer is aware of the private vehicle, bus, and ride-hailing demand for the upcoming 650τ duration. However, after every update step of $\tilde{T} = 200$ time steps, we reinitialize the MPC dynamics with the actual state variables for the model dynamics with abandonment to bridge the gap between the MPC predictions and the actual network dynamics.

With slightly higher objective function value of 184884 pax.hr, the MPC framework with two decision variables ϕ_V and ϕ_B generally performs better with significantly fewer abandonment compared to the MPC framework with one decision variable ϕ_V where the total delays yield a value of 184691 pax.hr but the abandoning requests are significantly larger. Again, this accentuates the importance of pooling, even in the vehicle network, which significantly reduces waiting times, and improves empty vehicle availability.

As in Figure 9, the results of the MPC with one control variable are shown in Figure 11, in addition to the variation of the cumulative abandoning requests in Figure 11(j). Clearly, the number of abandoning ride-hailing requests increases during peak hours, yet the variation of the decision variable ϕ_V in Figures 9(i) and 11(i) are almost similar. To conclude, this strategy therefore has a positive influence on the service level of ride-hailing platforms, even if the question here arises on which party should bear the incentivizing fare for pooling.

V. CONCLUSIONS

In this work, we develop an aggregate dynamic for a multi-modal network with private vehicles, ride-hailing services, and public transportation. Our modeling approach aims at evaluating an occupancy-dependent space allocation policy where a fraction of the pool ride-hailing users choose to utilize dedicated bus lanes. Despite ameliorating the total user delays and the ride-hailing service levels, our allocation strategy is not capable by itself of modifying the selfish user choices that do not necessarily align with the network-level optimum. The

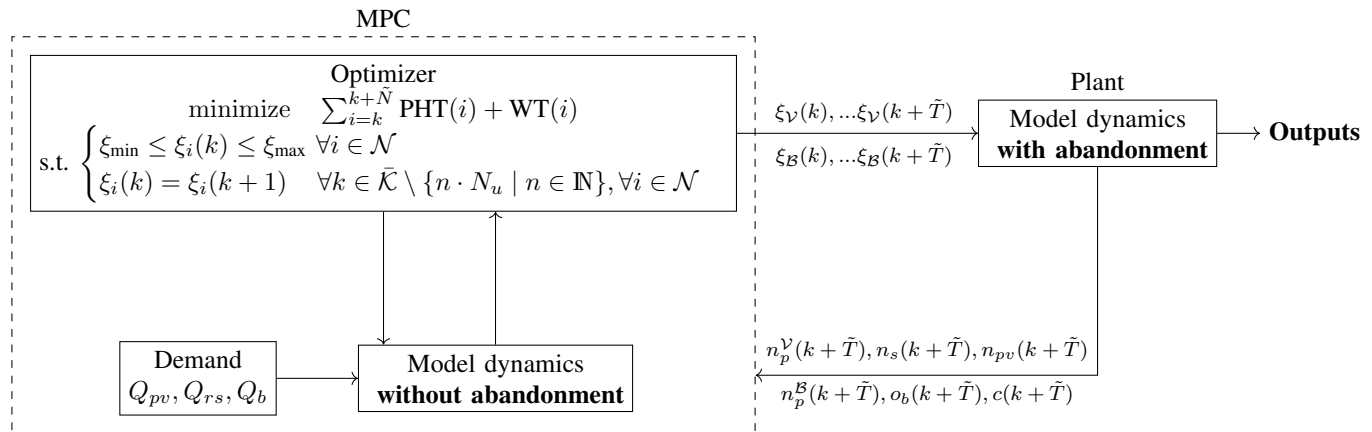


Fig. 10. Implementation of the MPC framework with abandonment. In this framework, the MPC dynamics run without abandonment with a prediction horizon of \tilde{N} whereas the plant dynamics run with abandonment. After every update step \tilde{T} , we reinitialize the MPC with some updated initial states retrieved from the plant dynamics.

TABLE IV
MACRO-SIMULATION RESULTS WITH ABANDONMENT

Scenario	PHT+WT [pax.hr]	Abandonment [pax]
$\beta_V = 0$ & $\beta_B = 0$	211898	17816
$\beta_V \in [0, 1]$ & $\beta_B = 0$	210505	15970
$\beta_V = 0$ & $\beta_B \in [0, 1]$	185664	4812
$\beta_V = 0$ & $\beta_B = 1$	196565	12630
$\beta_V \in [0, 1]$ & $\beta_B \in [0, 1]$	185157	4732
PI control - ϕ_B	186471	5398
MPC - ϕ_B	184691	4665
MPC - ϕ_V and ϕ_B	184884	3979

TABLE V
MULTI-MODAL DELAYS

Scenario	PHT _{pv} [pax.hr]	PHT _{rs} [pax.hr]	PHT _b [pax.hr]
$\beta_V = 0$ & $\beta_B = 0$	114856	17815	65578
$\beta_V \in [0, 1]$ & $\beta_B = 0$	114855	21367	65058
$\beta_V = 0$ & $\beta_B \in [0, 1]$	84902	19811	72407
$\beta_V = 0$ & $\beta_B = 1$	77072	24039	87451
$\beta_V \in [0, 1]$ & $\beta_B \in [0, 1]$	88282	20504	69169
PI control - ϕ_B	89558	20587	69086
MPC - ϕ_B	88494	20479	68444
MPC - ϕ_V and ϕ_B	88409	20637	68335

need for a more elaborate pricing scheme to steer the user's choice towards a more convenient solution for multi-modal users is therefore substantiated. Consequently, we build both a PI and an MPC control framework, and analyze what the additional pooling discount or fare should be that improves the overall travel times for all network users, and the waiting time for ride-hailing users in specific. Our results show that pricing indeed influences the preferences of ride-hailing requests in a manner that reduces the PHT for all modes. We performed the same analysis for the cases with and without request abandonment, and demonstrated how the complexity of our abandonment function is circumvented in the MPC solution.

In future work, we plan to give further attention to demand-dependent trip detours. This is because the detour distance itself for a pool trip is lower when more passengers opt for pooling. Therefore, the efficiency of our proposed policy

becomes more accentuated if this factor is accounted for in the modeling formulation. Moreover, we have considered so far pool trips with only two passengers sharing their rides. A potential direction for this work is to extend this work to incorporate a high-capacity on-demand micro-transit service utilizing the bus network along with buses, and observe the additional occupancy-dependent improvements that we achieve if these services progressively gain more and more momentum.

REFERENCES

- [1] L. Fayed, G. Nilsson, and N. Geroliminis, "A macroscopic modelling framework for the dynamic pricing of pool ride-splitting vehicles in bus lanes," 2023, Accepted to The 26th IEEE International Conference on Intelligent Transportation Systems. IEEE ITSC.
- [2] S. Shaheen, A. Bansal, N. Chan, and A. Cohen, "Mobility and the sharing economy: Industry developments and early understanding of impacts," *Low Carbon Mobility for Future Cities*, 2017.
- [3] G. Erhardt, S. Roy, D. Cooper, B. Sana, M. Chen, and J. Castiglione, "Do transportation network companies decrease or increase congestion?" *Science Advances*, vol. 5, p. eaau2670, 2019.
- [4] C. V. Beojone and N. Geroliminis, "On the inefficiency of ride-sourcing services towards urban congestion," *Transportation Research Part C: Emerging Technologies*, vol. 124, p. 102890, 2021.
- [5] L. A. de Souza Silva, M. O. de Andrade, and M. L. Alves Maia, "How does the ride-hailing systems demand affect individual transport regulation?" *Research in Transportation Economics*, vol. 69, pp. 600–606, 2018.
- [6] A. Tirachini and A. Gómez-Lobo, "Does ride-hailing increase or decrease vehicle kilometers traveled (VKT)? A simulation approach for Santiago de Chile," *International Journal of Sustainable Transportation*, vol. 14, pp. 1–18, 2019.
- [7] S. Li, J. Qin, H. Yang, K. Poolla, and P. Varaiya, "Off-street parking for TNC vehicles to reduce cruising traffic," *2020 59th IEEE Conference on Decision and Control (CDC)*, pp. 2585–2590, 2020.
- [8] Z. Xu, Y. Yin, and L. Zha, "Optimal parking provision for ride-sourcing services," *Transportation Research Part B: Methodological*, vol. 105, pp. 559–578, 2017.
- [9] J. J. Yu, C. S. Tang, Z.-J. Max Shen, and X. M. Chen, "A balancing act of regulating on-demand ride services," *Management Science*, vol. 66, no. 7, pp. 2975–2992, 2020.
- [10] L. Zha, Y. Yin, and H. Yang, "Economic analysis of ride-sourcing markets," *Transportation Research Part C: Emerging Technologies*, vol. 71, pp. 249–266, 2016.
- [11] J. Ke, H. Yang, X. Li, H. Wang, and J. Ye, "Pricing and equilibrium in on-demand ride-pooling markets," *Transportation Research Part B: Methodological*, vol. 139, pp. 411–431, 2020.

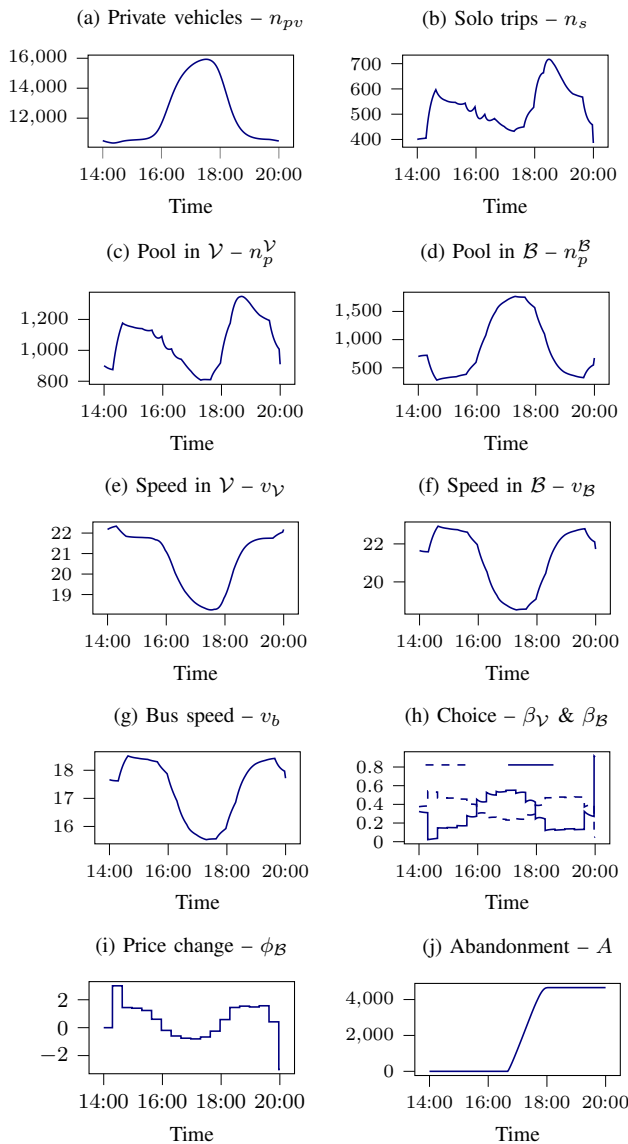


Fig. 11. Time-dependent model variables for the MPC framework with abandonment for (a) private vehicle accumulation, (b) solo trip ride-hailing vehicles, (c) pool trip ride-hailing accumulation in \mathcal{V} , (d) pool trip ride-hailing accumulation in \mathcal{B} , (e) speed in the vehicle network \mathcal{V} , (f) vehicle speed in the bus network \mathcal{B} , (g) bus speed in the bus network \mathcal{B} , (h) fraction of pool trip in \mathcal{V} and \mathcal{B} respectively, (i) regulatory control fare for pooling in \mathcal{B} , and (j) cumulative abandoning requests.

- [12] J. Ke, Z. Zheng, H. Yang, and J. Ye, "Data-driven analysis on matching probability, routing distance and detour distance in ride-pooling services," *Transportation Research Part C: Emerging Technologies*, vol. 124, p. 102922, 2021.
- [13] S. Ma, Y. Zheng, and O. Wolfson, "Real-time city-scale taxi ridesharing," *IEEE Transactions on Knowledge and Data Engineering*, vol. 27, pp. 1782–1795, 2015.
- [14] S. Shaheen and A. Cohen, "Shared ride services in North America: Definitions, impacts, and the future of pooling," *Transport Reviews*, vol. 39, no. 4, pp. 427–442, 2019.
- [15] A. Tirachini, "Ride-hailing, travel behaviour and sustainable mobility: An international review," *Transportation*, vol. 47, 2020.
- [16] J. Cramer and A. B. Krueger, "Disruptive change in the taxi business: The case of Uber," *American Economic Review*, vol. 106, no. 5, pp. 177–82, 2016.
- [17] J. C. Castillo, D. Knoepfle, and G. Weyl, "Surge pricing solves the wild goose chase," in *Proceedings of the 2017 ACM Conference on Economics and Computation*, ser. EC '17. New York, NY, USA: Association for Computing Machinery, 2017, p. 241–242.
- [18] Z. Xu, Y. Yin, and J. Ye, "On the supply curve of ride-hailing systems," *Transportation Research Part B: Methodological*, vol. 132, pp. 29–43, 2020, 23rd International Symposium on Transportation and Traffic Theory (ISTTT 23).
- [19] G. P. Cachon, K. M. Daniels, and R. Lobel, "The role of surge pricing on a service platform with self-scheduling capacity," *Manufacturing & Service Operations Management*, vol. 19, no. 3, pp. 368–384, 2017.
- [20] K. Zhang and Y. M. Nie, "To pool or not to pool: Equilibrium, pricing and regulation," *Transportation Research Part B: Methodological*, vol. 151, pp. 59–90, 2021.
- [21] M. Nourinejad and M. Ramezani, "Ride-sourcing modeling and pricing in non-equilibrium two-sided markets," *Transportation Research Part B: Methodological*, vol. 132, pp. 340–357, 2020, 23rd International Symposium on Transportation and Traffic Theory (ISTTT 23).
- [22] L. Zha, Y. Yin, and Z. Xu, "Geometric matching and spatial pricing in ride-sourcing markets," *Transportation Research Part C: Emerging Technologies*, vol. 92, pp. 58–75, 2018.
- [23] K. Bimpikis, O. Candogan, and D. Saban, "Spatial pricing in ride-sharing networks," *Operations Research*, vol. 67, no. 3, pp. 744–769, 2019.
- [24] M. Ramezani and A. H. Valadkhani, "Dynamic ride-sourcing systems for city-scale networks - Part I: Matching design and model formulation and validation," *Transportation Research Part C: Emerging Technologies*, vol. 152, p. 104158, 2023.
- [25] A. H. Valadkhani and M. Ramezani, "Dynamic ride-sourcing systems for city-scale networks, Part ii: Proactive vehicle repositioning," *Transportation Research Part C: Emerging Technologies*, vol. 152, p. 104159, 2023.
- [26] R. Tachet, O. Sagarra, P. Santi, G. Resta, M. Szell, S. Strogatz, and C. Ratti, "Scaling law of urban ride sharing," *Scientific Reports*, 10 2016.
- [27] J. Soza-Parra, R. Kucharski, and O. Cats, "The shareability potential of ride-pooling under alternative spatial demand patterns," *Transportmetrica A Transport Science*, 2023.
- [28] J. Jung, R. Jayakrishnan, and J. Y. Park, "Dynamic shared-taxi dispatch algorithm with hybrid-simulated annealing," *Computer-Aided Civil and Infrastructure Engineering*, vol. 31, no. 4, pp. 275–291, 2016.
- [29] D. O. Santos and E. C. Xavier, "Dynamic taxi and ridesharing: A framework and heuristics for the optimization problem," in *Proceedings of the Twenty-Third International Joint Conference on Artificial Intelligence*, ser. IJCAI '13. AAAI Press, 2013, p. 2885–2891.
- [30] J. Alonso-Mora, S. Samaranayake, A. Wallar, E. Frazzoli, and D. Rus, "On-demand high-capacity ride-sharing via dynamic trip-vehicle assignment," *Proceedings of the National Academy of Sciences*, vol. 114, p. 201611675, 01 2017.
- [31] J. Wang, X. Wang, S. Yang, H. Yang, X. Zhang, and Z. Gao, "Predicting the matching probability and the expected ride/shared distance for each dynamic ridepooling order: A mathematical modeling approach," *Transportation Research Part B: Methodological*, vol. 154, pp. 125–146, 2021.
- [32] J. D. Hall, C. Palsson, and J. Price, "Is Uber a substitute or complement for public transit?" *Journal of Urban Economics*, vol. 108, pp. 36–50, 2018.
- [33] J. Ke, Z. Zhu, H. Yang, and Q. He, "Equilibrium analyses and operational designs of a coupled market with substitutive and complementary ride-sourcing services to public transits," *Transportation Research Part E: Logistics and Transportation Review*, vol. 148, p. 102236, 2021.
- [34] Z. Zhu, A. Xu, Q.-C. He, and H. Yang, "Competition between the transportation network company and the government with subsidies to public transit riders," *Transportation Research Part E: Logistics and Transportation Review*, vol. 152, p. 102426, 2021.
- [35] M. Ma, Y. Chen, W. Liu, and S. T. Waller, "An economic analysis of a multi-modal transportation system with ride-sourcing services and multi-class users," *Transport Policy*, vol. 140, pp. 1–17, 2023.
- [36] T. Toledo, O. Mansour, and J. Haddad, "Optimal dynamic tolls for managed lanes," *Transportation Research Record: Journal of the Transportation Research Board*, vol. 2606, pp. 28–37, 2017.
- [37] M. C. Cohen, A. Jacquillat, A. Ratzon, and R. Sasson, "The impact of high-occupancy vehicle lanes on carpooling," *Transportation Research Part A: Policy and Practice*, vol. 165, pp. 186–206, 2022.
- [38] R. Lamotte, A. de Palma, and N. Geroliminis, "On the use of reservation-based autonomous vehicles for demand management," *Transportation Research Part B: Methodological*, vol. 99, pp. 205–227, 2017.
- [39] D. Tsitsokas, A. Kouvelas, and N. Geroliminis, "Modeling and optimization of dedicated bus lanes space allocation in large networks

- with dynamic congestion,” *Transportation Research Part C: Emerging Technologies*, vol. 127, p. 103082, 2021.
- [40] L. Fayed, G. Nilsson, and N. Geroliminis, “On the utilization of dedicated bus lanes for pooled ride-hailing services,” *Transportation Research Part B: Methodological*, vol. 169, pp. 29–52, 2023.
 - [41] N. Geroliminis and C. F. Daganzo, “Existence of urban-scale macroscopic fundamental diagrams: Some experimental findings,” *Transportation Research Part B: Methodological*, vol. 42, no. 9, pp. 759–770, 2008.
 - [42] W. Ni and M. Cassidy, “City-wide traffic control: Modeling impacts of cordon queues,” *Transportation Research Part C: Emerging Technologies*, vol. 113, 2019.
 - [43] I. I. Sirmatel, D. Tsitsokas, A. Kouvelas, and N. Geroliminis, “Modeling, estimation, and control in large-scale urban road networks with remaining travel distance dynamics,” *Transportation Research Part C: Emerging Technologies*, 2021.
 - [44] N. Geroliminis, N. Zheng, and K. Ampountolas, “A three-dimensional macroscopic fundamental diagram for mixed bi-modal urban networks,” *Transportation Research Part C: Emerging Technologies*, vol. 42, pp. 168–181, 2014.

This figure "mpc_one.png" is available in "png" format from:

<http://arxiv.org/ps/2310.01286v1>

This figure "mpc_two.png" is available in "png" format from:

<http://arxiv.org/ps/2310.01286v1>